

# Deep Retinex Network for Estimating Illumination Colors with Self-Supervised Learning

1<sup>st</sup> Kouki Seo  
Department of Computer Science  
Tokyo Metropolitan University  
Tokyo, Japan  
seo-kouki@ed.tmu.ac.jp

2<sup>nd</sup> Yuma Kinoshita  
Department of Computer Science  
Tokyo Metropolitan University  
Tokyo, Japan  
ykinoshita@tmu.ac.jp

3<sup>rd</sup> Hitoshi Kiya  
Department of Computer Science  
Tokyo Metropolitan University  
Tokyo, Japan  
kiya@tmu.ac.jp

**Abstract**—We propose a novel Retinex image-decomposition network that can be trained in a self-supervised manner. The Retinex image-decomposition aims to decompose an image into illumination-invariant and illumination-variant components, referred to as “reflectance” and “shading,” respectively. Although there are three consistencies that the reflectance and shading should satisfy, most conventional work considers only one or two of the consistencies. For this reason, the three consistencies are considered in the proposed network. In addition, by using generated pseudo-images for training, the proposed network can be trained with self-supervised learning. Experimental results show that our network can decompose images into reflectance and shading components. Furthermore, it is shown that the proposed network can be used for white-balance adjustment.

**Index Terms**—Retinex decomposition, intrinsic image decomposition, white balance, self-supervised learning

## I. INTRODUCTION

A natural image consists of the reflectance and the shading of a scene in Retinex theory [1]. The reflectance and the shading are an illumination-invariant component and an illumination-variant component respectively. Retinex image decomposition aims to decompose a natural image into two such components. To enable the decomposition, various methods have so far been proposed [2]–[10], where most methods are based on deep neural networks (DNN).

In the Retinex decomposition, there are three premises regard to consistency: reconstruction consistency, reflectance consistency in terms of exposures, and reflectance consistency in terms of illumination colors. However, most conventional methods only considers some of them. In contrast, conventional methods [4], [5] consider all of the premises, but their performances are limited due to difficulty in preparing a large amount of real data or synthetic data for training.

Several decomposition methods trained with supervised learning have been proposed [7]–[10]. They often use a highly-synthetic dataset or a human-labeled dataset of the real scene [11]–[13]. However, such datasets are insufficient to generalize real scenes.

To solve these problems, in this paper, we propose a novel Retinex image decomposition network that considers both the three premises and the problem with data. For training the proposed network, we generate pseudo images that are taken under various exposure and illumination-color conditions. By

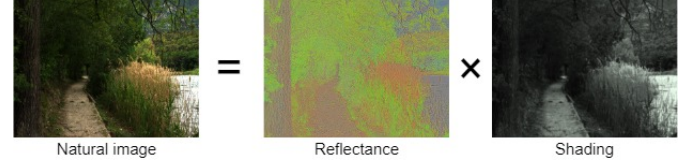


Fig. 1. Retinex image decomposition.

using such training data, the proposed network can be trained with self-supervised learning, and difficulty in preparing a large amount of data can be overcome. The proposed network can decompose input image  $I$  into reflectance  $R_I$ , gray-shading  $GS_I$ , and single RGB vector  $c_I$  that represents an illumination color. Shading  $S_I$  including the effect of illumination color can be obtained by multiplying outputs  $GS_I$  and  $c_I$ .

We evaluate the performance of the decomposition and the estimation of illumination colors in terms of mean squared error (MSE) and hue difference  $\Delta H$  of CIEDE2000 [15]. Experimental results show that our network can decompose input images, and identify illumination colors of the input images.

## II. PRELIMINARIES

### A. Retinex decomposition

In Retinex theory, a natural image  $I$  can be written as the pixel-wise product of reflectance  $R_I$  and shading  $S_I$  as shown in Fig. 1, i.e.,

$$I(x, y) = R_I(x, y) \cdot S_I(x, y), \quad (1)$$

where  $(x, y)$  indicates a pixel coordinate,  $R_I(x, y)$  is in the range of  $[0, 1]$ , and  $S_I(x, y)$  is in the range of  $[0, \infty)$ . The goal of Retinex decomposition is to estimate reflectance  $R_I$  and shading  $S_I$  from a given image  $I$ . Here, shading  $S$  will be spatially smooth because it is a map of the illumination intensity. In contrast, since  $R$  is expected to include textures and edges of objects, reflectance  $R$  will be spatially discontinuous.

### B. Effects of exposure change on Retinex decomposition

The change of the brightness (or exposure) of an image affects the Retinex decomposition of the image. Here, we discuss the effects of the exposure change.

The exposure of an image is usually expressed in terms of an exposure value (EV), and the proper exposure for a scene is automatically decided by a camera [16]–[19]. The exposure value is commonly controlled by changing the shutter speed, although it can also be controlled by adjusting various camera parameters. Here, we assume that camera parameters except for the shutter speed are fixed. Let  $v_0 = 0[\text{EV}]$  and  $I_{v_0}$  be the proper exposure value and the corresponding captured image under the given conditions, respectively. By assuming that the camera response is linear with respect to the light intensity, an image  $I_{v_i}$  exposed at  $v_i[\text{EV}]$  is written as

$$I_{v_i}(x, y) = 2^{v_i} I_{v_0}(x, y). \quad (2)$$

From Eqs. (1) and (2), the Retinex decomposition of  $I_{EV=v_0}$  and  $I_{EV=v_i}$  are given as

$$I_{v_0}(x, y) = R_{I_{v_0}}(x, y) \cdot S_{I_{v_0}}(x, y), \quad (3)$$

$$\begin{aligned} I_{v_i}(x, y) &= R_{I_{v_i}}(x, y) \cdot S_{I_{v_i}}(x, y) \\ &= 2^{v_i} R_{I_{v_0}}(x, y) \cdot S_{I_{v_0}}(x, y), \end{aligned} \quad (4)$$

respectively. Since the scenes of images  $I_{v_0}$  and  $I_{v_i}$  are the same, we can obtain the following relations:

$$R_{I_{v_i}} = R_{I_{v_0}}, \quad (5)$$

$$S_{I_{v_i}} = 2^{v_i} S_{I_{v_0}}. \quad (6)$$

### C. Effects of illumination color on Retinex decomposition

Similarly to the exposure change, the change of illumination color also affects shading  $S_I$ .

Let  $\mathbf{c}_0 = (1, 1, 1)$ ,  $I_{\mathbf{c}_0}$ , and  $S_{I_{\mathbf{c}_0}}$  be the white illumination color, an image taken under the illumination, and its corresponding shading, respectively. Then, shading  $S_{I_{\mathbf{c}_j}}$  corresponding to  $I_{\mathbf{c}_j}$  taken under illumination color  $\mathbf{c}_j = (r, g, b)$  is given as

$$S_{I_{\mathbf{c}_j}}(x, y) = \mathbf{M}_{\mathbf{c}_j} S_{I_{\mathbf{c}_0}}(x, y), \quad (7)$$

where  $\mathbf{M}_{\mathbf{c}_j} = \text{diag}(\mathbf{c}_j)$ . For this reason, the Retinex decomposition of  $I_{\mathbf{c}_0}$  and  $I_{\mathbf{c}_j}$  is given by

$$I_{\mathbf{c}_0}(x, y) = \text{diag}(R_{I_{\mathbf{c}_0}}(x, y)) S_{I_{\mathbf{c}_0}}(x, y), \quad (8)$$

$$\begin{aligned} I_{\mathbf{c}_j}(x, y) &= \text{diag}(R_{I_{\mathbf{c}_j}}(x, y)) S_{I_{\mathbf{c}_j}}(x, y) \\ &= \text{diag}(R_{I_{\mathbf{c}_0}}(x, y)) \mathbf{M}_{\mathbf{c}_j} S_{I_{\mathbf{c}_0}}(x, y) \\ &= \mathbf{M}_{\mathbf{c}_j} \text{diag}(R_{I_{\mathbf{c}_0}}(x, y)) S_{I_{\mathbf{c}_0}}(x, y), \end{aligned} \quad (9)$$

where we used the relation

$$R_{I_{\mathbf{c}_j}} = R_{I_{\mathbf{c}_0}}. \quad (10)$$

Therefore, the relationship between  $I_{\mathbf{c}_0}$  and  $I_{\mathbf{c}_j}$  is written as

$$I_{\mathbf{c}_j}(x, y) = \mathbf{M}_{\mathbf{c}_j} I_{\mathbf{c}_0}(x, y). \quad (11)$$

### D. Scenario

In the Retinex decomposition, there are three premises:

**Reconstruction consistency** The product of estimated reflectance and shading matches the corresponding original image, as shown in Eq. (1).

**Reflectance consistency (exposure)** Reflectances are invariant against a change of exposure values, as in Eq. (5).

**Reflectance consistency (color)** Reflectances are invariant against a change of illumination colors, as in Eq. (10).

Most conventional work considers only a part of these premises, e.g., reconstruction consistency and reflectance consistency (exposure). In such a case, their reflectance components are affected by the effects of exposure and illumination-color conditions. In literature [4], all three premises are considered by training a DNN by using videos taken by a fixed-point camera. However, the DNN still has a limited performance due to a limited amount of real data for training.

For these reasons, in this paper, we propose a novel DNN for the Retinex decomposition considering all three premises and the problem with data. For training our network, we generate pseudo images from original images, which correspond to images taken under various exposure and illumination-color conditions. By using them, our network can be trained with self-supervised learning while considering above three premises. In addition, since we generate pseudo images from general datasets, the problem with a amount of data can be overcome.

## III. PROPOSED RETINEX NETWORK

In this paper, we aim to decompose image  $I$  into reflectance  $R_I$  and shading  $S_I$  by using a deep neural network. The key idea of our approach is to consider the three premises in section II-D. The proposed network can be trained in a self-supervised manner, while satisfying the premises.

### A. Network architecture

Figure 2 illustrates the architecture of the proposed network. The proposed network receives input image  $I$ , and outputs reflectance  $R_I$ , gray-shading  $GS_I$ , and RGB vector  $\mathbf{c}_I$ . Our network has a single encoder and three decoders. By the encoder, input image  $I$  is transformed into feature maps that will be fed into decoders. Reflectance  $R_I$  with RGB color channels is directly obtained as the output of a decoder. In contrast, shading  $S_I$  is given as the product of RGB vector  $\mathbf{c}_I$  and gray-scale shading  $GS_I$ . The gray-scale shading and the RGB vector are outputted from the other two decoders, respectively.

### B. Data generation for self-supervised learning

In order to consider the three premises in Section II-D, images of a single scene taken under various exposure and illumination-color conditions are required for training the proposed network. However, it is very costly to collect such images. For this reason, we generate pseudo images from raw images and use them for training the proposed network.

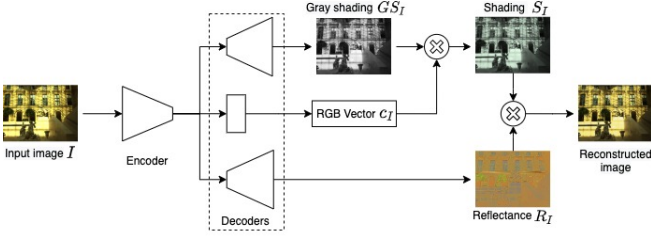


Fig. 2. Network architecture

Because raw images are not affected by the non-linear camera response of a camera, multiplying their pixel values by a scalar value corresponds to the exposure change in Eq. (2). In addition, Eq. (11) is equivalent to applying a color-transfer matrix, used in a white-balance adjustment in the RGB color space, to an image. Hence, images generated from raw images in accordance with Eqs. (12) and (13) can be used for training the proposed network.

We utilize three color-transferred multi-exposure images  $I_{v_i, c_i}$  ( $i \in \{1, 2, 3\}$ ) having exposure value  $v_i$  and illumination color  $c_i$  for calculating loss. Images  $I_{v_i, c_i}$  are generated from a raw image  $I_{\text{raw}}$  as follows:

- 1) Obtain an RGB image  $I_{\text{RGB}}$  by demosaicing a raw image  $I_{\text{raw}}$ .
- 2) Generate three multi-exposure images  $I_{v_i}$  ( $v_i \in \{-1, 0, 1\}$  [EV]) from  $I_{\text{RGB}}$  in accordance with Eq.(2) as

$$I_{v_i} = 2^{v_i} \frac{0.18}{g(I_{\text{RGB}})} I_{\text{RGB}}, \quad (12)$$

where  $g(I_{\text{RGB}})$  indicates the geometric mean of the luminance of  $I_{\text{RGB}}$ .

- 3) Generate color-transferred multi-exposure images  $I_{v_i, c_i}$  by multiplying  $I_{v_i}$  by  $M_{c_i} = \text{diag}(c_i)$  as

$$I_{v_i, c_i} = M_{c_i} I_{v_i}, \quad (13)$$

where  $c_i$  is a random vector in  $[0.9, 1.1]^3$ .

### C. Loss functions

To fulfill above premises, our network is trained to minimize the following loss function

$$\mathcal{L} = \mathcal{L}_{\text{recon}} + \mathcal{L}_{\text{reflect}} + \mathcal{L}_{\text{other}}, \quad (14)$$

where  $\mathcal{L}_{\text{recon}}$  is the image-reconstruction loss between input images and reconstructed ones.  $\mathcal{L}_{\text{reflect}}$  and  $\mathcal{L}_{\text{other}}$  are loss functions for constraining outputs  $\hat{R}_{I_i}$ , and  $\hat{S}_{I_i}$  and  $\hat{c}_{I_i}$ , respectively.

For the reconstruction consistency, in accordance with Eq.(1), we use image-reconstruction loss  $\mathcal{L}_{\text{recon}}$  so that the pixel product of  $\hat{R}_{I_i}(x, y)$  and  $\hat{S}_{I_i}(x, y)$  is equal to input image

$I_i \triangleq I_{v_i, c_i}$ . We calculate  $\mathcal{L}_{\text{recon}}$  for all combinations of the input images and the pixel product  $\hat{R}_{I_i}(x, y) \cdot \hat{S}_{I_i}(x, y)$  as

$$\begin{aligned} \mathcal{L}_{\text{recon}} = & \sum_{i=1}^3 \sum_{j=1}^3 \{ \lambda_1 \|I_i(x, y) - \hat{R}_{I_j}(x, y) \cdot \hat{S}_{I_i}(x, y)\|^2 \\ & + \lambda_2 \|1 - \text{SSIM}(I_i(x, y), \hat{R}_{I_j}(x, y) \cdot \hat{S}_{I_i}(x, y))\|^2 \\ & + \lambda_3 \|\Delta E(I_i(x, y), \hat{R}_{I_j}(x, y) \cdot \hat{S}_{I_i}(x, y))\|^2 \}, \end{aligned} \quad (15)$$

where  $\lambda_1, \lambda_2$  and  $\lambda_3$  are weights of the loss terms,  $\|\cdot\|$  is L2 norm,  $\text{SSIM}(\cdot)$  calculates a structural similarity (SSIM) value, and  $\Delta E(\cdot)$  calculates the CIEDE2000 color difference [15]. By using SSIM and  $\Delta E(\cdot)$  as the loss terms, images reconstructed by using outputs  $\hat{R}_{I_i}$  and  $\hat{S}_{I_i}$  reproduce the details of input images  $I_i$ , and moreover output reflectance  $\hat{R}_{I_i}$  can be consistent regardless of exposure and illumination-color conditions.

Also, we use reflectance loss  $\mathcal{L}_{\text{reflect}}$  to improve the consistency of output reflectance  $\hat{R}_{I_i}$  as

$$\begin{aligned} \mathcal{L}_{\text{reflect}} = & \sum_{i=1}^3 \sum_{j=1}^3 \{ \lambda_4 \|\hat{R}_{I_i}(x, y) - \hat{R}_{I_j}(x, y)\|^2 \\ & + \lambda_5 |0.5 - \text{mean}(\hat{R}_{I_i})| \}, \end{aligned} \quad (16)$$

where  $\lambda_4$  and  $\lambda_5$  are weights of the loss terms,  $\text{mean}(\cdot)$  calculates the mean value of the whole reflectance. By adjusting the mean value to 0.5, our network can output the normalized color information of input images  $I_i$  as reflectance  $\hat{R}_{I_i}$ .

To add smoothness to output shading  $\hat{S}_{I_i}$ , the total variation  $\text{tv}(\cdot)$  is utilized as a loss function for shading. Combining  $\text{tv}(\cdot)$  and a loss function of output RGB vector  $\hat{c}_{I_i}$ , we calculate  $\mathcal{L}_{\text{other}}$  as follows:

$$\mathcal{L}_{\text{other}} = \sum_{i=1}^3 \{ \lambda_6 \text{tv}(\hat{S}_{I_i}) + \lambda_7 \|c_i - \hat{c}_{I_i}\|^2 \}, \quad (17)$$

where  $\lambda_6$  and  $\lambda_7$  are weights of the loss terms.

In practice, we empirically set  $\lambda_1 = 3, \lambda_2 = 1, \lambda_3 = 2, \lambda_4 = 3, \lambda_5 = 1, \lambda_6 = 10$  and  $\lambda_7 = 20$  as weights, respectively.

## IV. SIMULATION

We performed two simulations to confirm the performance of the proposed network. For training our network, we used 3640 raw images in the HDR+ Burst Photography Dataset [20].

### A. Result of Retinex Decomposition

Figure 3 shows an example of images outputted from our network as Retinex decomposition and reconstruction. From Fig.3, our network was confirmed to generate almost the same reflectance from three input images with different exposures. Figure 3 also shows that the input images with different exposures were able to be reconstructed by using output components. From these results, our network was demonstrated to work well.

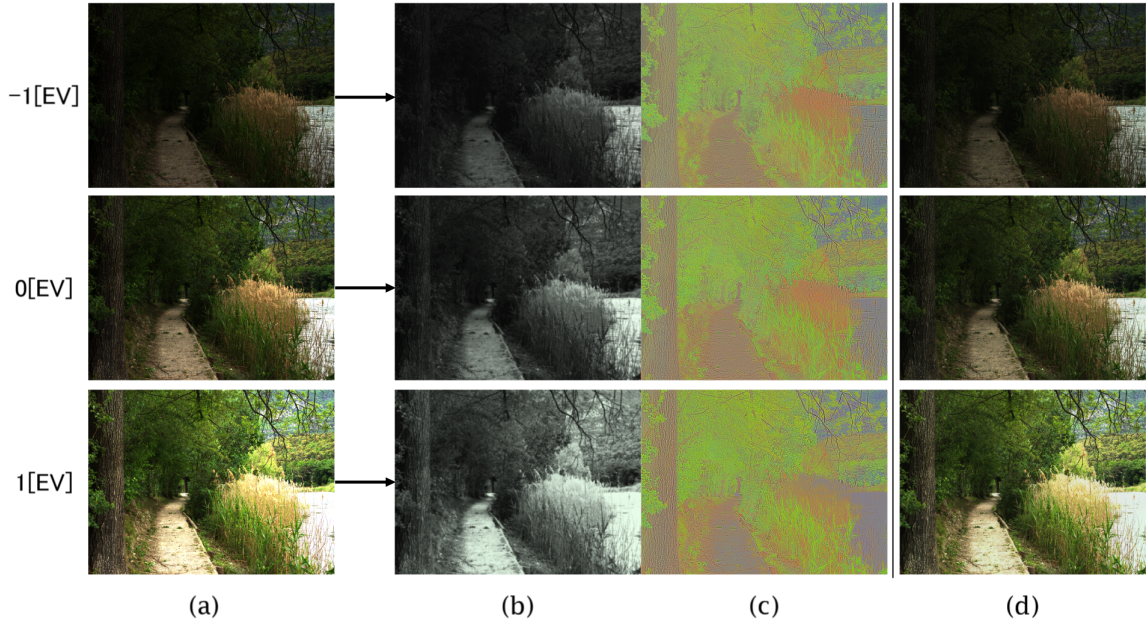


Fig. 3. Example of images generated by our network. (a) Input image. (b) Output shading. (c) Output reflectance. (d) Reconstructed image by using output components.

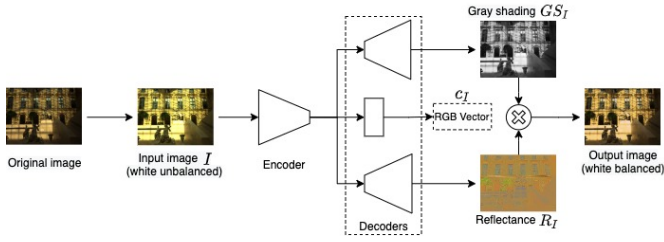


Fig. 4. WB adjustment with our network

### B. Result of white-balance adjustment

To evaluate the estimation performance of illumination colors, a WB adjustment was applied to input images, where the input images were prepared as white unbalanced images by using only color-transferring, i.e. using steps (1) and (3) in Sec.III-B. Figure 4 shows the process of the WB adjustment used in this experiment. In the process, outputted RGB vectors were not used for reconstructing output images so that the effects of the illumination color included in input images were eliminated from the images.

In this experiment, 100 color-transferred images, which were generated from 100 raw images in the RAISE Dataset [21], were applied to the trained network as input images. Output images produced from the proposed network were evaluated in terms of MSE and hue difference  $\Delta H$  of CIEDE2000 [15]. To confirm the decomposition performance of our network, the scores of output images were compared with those of input ones, where original images that were not color-transferred were used as reference ones for calculating scores.

TABLE I  
SCORES OF WB ADJUSTMENT SIMULATION.

	MSE	$\Delta H$
Input	0.0259	3.5017
Output	<b>0.0198</b>	<b>3.2403</b>



(a) Original image (Reference)



(b) Input image



(c) Output image

Fig. 5. Example of WB adjustment with out network

Table I shows the scores of MSE and hue difference  $\Delta H$ , which were averaged over all 100 images. From Table I, both scores of the output images were lower than those of the input images, where a smaller value indicates a better result in the scores. Figure 5 shows an example of the reference, input, and output images used in this experiment. From Fig.5, the white



balance of the output image was closer to the reference one than the input one. Therefore, our network was confirmed to be able to eliminate the effects of the illumination color of the input image.

## V. CONCLUSION

In this paper, we proposed a novel Retinex image decomposition network considering the premises of the Retinex decomposition. In addition, the proposed network can be trained in a self-supervised manner by using pseudo-generated images with various exposures and illumination colors. In an experiment, our network was demonstrated to be able to generate almost the same reflectance from input images with different exposures and estimate illumination colors.

## REFERENCES

- [1] E. H. Land, "The retinex theory of color vision," *Scientific american*, vol.237, no.6, pp.108–129, 1977.
- [2] C. Chien, Y. Kinoshita, S. Shiota, and H. Kiya, "A Retinex-based Image Enhancement Scheme with Noise Aware Shadow-up Function," *Proc. SPIE 11049, IWAIT*, pp.501–506, 2019.
- [3] Y. Liu, Y. Li, S. You, and F. Lu, "Unsupervised Learning for Intrinsic Image Decomposition from a Single Image," *Proc. CVPR*, pp.3248–3257, 2020.
- [4] Z. Li, and N. Snavely, "Learning Intrinsic Image Decomposition from Watching the World," *Proc. CVPR*, pp.9039–9048, 2018.
- [5] L. Lettry, K. Vanhoey, and L. Van Gool, "Unsupervised Deep Single-Image Intrinsic Decomposition using Illumination-Varying Image Sequences," *Computer Graphics Forum*, vol.37, no.7, pp.409–419, 2018.
- [6] W. Ma, H. Chu, B. Zhou, R. Urtasun, and A. Torralba, "Single image intrinsic decomposition without a single intrinsic image," *Proc. ECCV*, pp.201–217, 2018.
- [7] Q. Fan, J. Yang, G. Hua, B. Chen, and D. Wipf, "Revisiting deep intrinsic image decompositions," *Proc. CVPR*, pp.8944–8952, 2018.
- [8] T. Zhou, P. Krahenbuhl, and A. A. Efros, "Learning data-driven reflectance priors for intrinsic image decomposition," *Proc. ICCV*, pp.3469–3477, 2015.
- [9] Z. Li, and N. Snavely, "CGIntrinsics: Better Intrinsic Image Decomposition through Physically-Based Rendering," *Proc. ECCV*, pp.371–387, 2018.
- [10] Z. Wang, and F. Lu, "Single image intrinsic decomposition with discriminative feature encoding," *Proc. ICCVW*, 2019.
- [11] R. Grosse, M. K. Johnson, E. H. Adelson, and W. T. Freeman, "Ground truth dataset and baseline evaluations for intrinsic image algorithms," *Proc. ICCV*, pp.2335–2342, 2009.
- [12] D. J. Butler, J. Wulff, G. B. Stanley, and M. J. Black, "A naturalistic open source movie for optical flow evaluation," *Proc. ECCV*, pp.611–625, 2012.
- [13] S. Bell, K. Bala, and N. Snavely, "Intrinsic Images in the Wild," *ACM Trans. Graph.*, vol.33, no.4, 2014.
- [14] B. Kovacs, S. Bell, N. Snavely and K. Bala, "Shading Annotations in the Wild," *Proc. CVPR*, pp.6998–7007, 2017.
- [15] G. Sharma, W. Wu, and E. N. Dalal, "The CIEDE2000 color-difference formula: Implementation notes, supplementary test data, and mathematical observations," *Color Research & Application*, vol.30, no.1, pp.21–30, 2005.
- [16] Y. Kinoshita and H. Kiya, "Scene Segmentation-Based Luminance Adjustment for Multi-Exposure Image Fusion," *IEEE Trans. Image Processing*, vol.28, no.8, pp.4101–4116, 2019.
- [17] Y. Kinoshita, S. Shiota and H. Kiya, "Automatic Exposure Compensation for Multi-Exposure Image Fusion," *Proc. ICIP*, pp.883–887, 2018.
- [18] Y. Kinoshita and H. Kiya, "Automatic Exposure Compensation Using an Image Segmentation Method for Single-Image-Based Multi-Exposure Fusion," *APSIPA Trans. Signal and Information Processing*, vol.7, p.e22, 2018.
- [19] K. Seo, C. Go, Y. Kinoshita and H. Kiya, "Hue-Correction Scheme Considering Non-Linear Camera Response for Multi-Exposure Image Fusion," *IEICE Trans. Fundamentals*, vol.E103-A, no.12, pp.1562–1570, 2020.
- [20] S. W. Hasinoff, D. Sharlet, R. Geiss, A. Adams, J. T. Barron, F. Kainz, J. Chen and M. Levoy, "Burst photography for high dynamic range and low-light imaging on mobile cameras," *ACM Trans. Graph.*, vol.35, no.6, 2016.
- [21] D.-T. Dang-Nguyen, C. Pasquini, V. Conotter, G. Boato, "RAISE: A Raw Images Dataset for Digital Image Forensics," *ACM Multimedia Systems*, pp.219–224, 2015.